

OPTIMISATION OF CMOS COMPATIBLE MICROBOLOMETER DEVICE PERFORMANCE

W. Maclean, M. du Plessis and J. Schoeman*

* Carl and Emily Fuchs Institute for Microelectronics, Dept. of Electrical, Electronic & Computer Engineering, Corner of University Road and Lynnwood Road, University of Pretoria, Pretoria 0002, South Africa. E-mail: johan.schoeman@eng.up.ac.za

Abstract: Uncooled IR (infrared) microbolometer performance is greatly affected by the thermal properties associated with the structural layout of each design. Equations are derived in this article which make use of basic structural dimensions to predict the expected thermal conductance and thermal capacitance of a microbolometer device. These equations enable a microbolometer designer to determine the estimated thermal time constant of a design without performing complicated analytical calculations for each layer in the design. Calculation results shown indicate the effect structural changes have on the thermal time constant of microbolometer devices. These changes aid microbolometer designers in adjusting the layout of the device to change the thermal time constant to the desired value. Structural deviations that occur during manufacturing of microbolometers are calculated and the possible causes are discussed.

Key words: Uncooled infrared bolometer, thermal properties, thermal performance prediction.

1. INTRODUCTION

Microbolometer device fabrication has been substantially simplified with the advances in MEMS (Micro-electromechanical structures), such as thermally isolating micro structures created with a complementary metal oxide semiconductor (CMOS) process [1]. These devices are manufactured by performing various processing techniques after the CMOS process has been completed. These post CMOS processing techniques are performed at a low temperature, to maintain the integrity of the underlying CMOS circuit.

Different microbolometer designs are used to determine the relationship between structural differences and the thermal performance of these devices. Specifically designed test devices will be used to isolate structural differences and determine the effect each structural difference has on the thermal performance. These changes in performance are used to derive equations that can be used to predict the thermal properties of a microbolometer design based on basic structural dimensions [2].

Experimental measurements performed on manufactured microbolometer devices reveal material property and structural differences from expected design values. These differences are calculated and possible causes for these differences are considered.

2. DESIGN OF MICROBOLOMETER TEST DEVICES

The microbolometer device shown in figure 1, illustrates the basic layout of a microbolometer with all structural elements indicated. This article will investigate performance changes with alterations to the support leg width and length. Test devices which isolate a single structural change are used. In one set the support leg

width is kept constant and only the length is changed to determine the change in thermal performance associated. Another set of devices are then used where the support leg length is kept constant and only the width is changed. The range of support leg widths used are between $8 \mu\text{m}$ and $20 \mu\text{m}$, and support leg lengths are between $89 \mu\text{m}$ and $169 \mu\text{m}$.

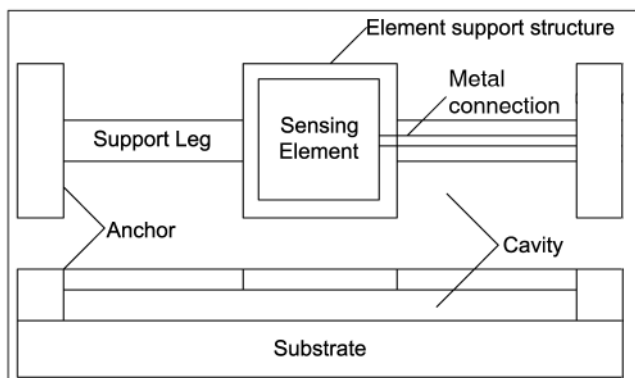


Figure 1: Basic structure of IR bolometer

Test structures used for the varying width test make use of an "I" bolometer design as shown in figure 1, bolometers used for the varying length test make use of an "L" design. The "L" design improves the shape of the microbolometer for integration in a FPA (Focal Plane Array) by keeping the device square whilst increasing the length of the support legs. FPAs are used to produce a two dimensional image from multiple microbolometers arranged in an array, connected to a readout circuit [3].

3. THERMAL PROPERTY CALCULATIONS

Thermal conductance defines the rate at which heat is transferred from the bolometer membrane throughout the

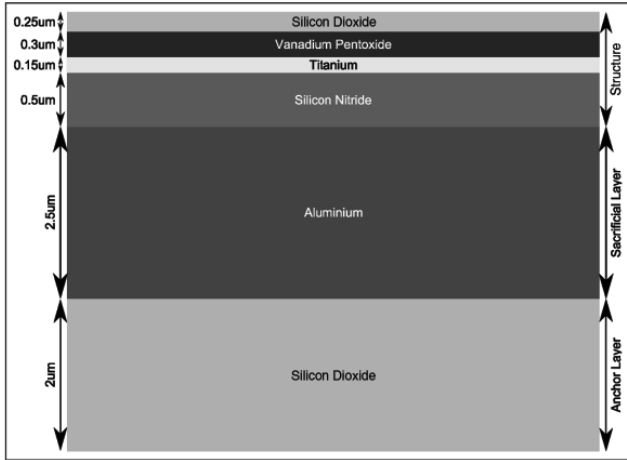


Figure 2: Material layers used for test devices

device and to the anchors which operate as heat sinks for the microbolometer device. The thermal conductance of a microbolometer can be calculated by using equation 1, where the three terms represent the physical thermal conductance, radiation thermal conductance and gaseous thermal conductance respectively [4, 5]. Devices packaged in a vacuum will have no conductance caused by gaseous thermal conductance and therefore equation 1 has to be changed accordingly.

$$G = \lambda \left(\frac{WT}{L} \right) + 4\delta\varepsilon A(Tm)^3 + \lambda_{air} \frac{A}{d}, \quad (1)$$

where:

λ = the thermal conductivity in W/mK

W = the width of the support legs in m

T = the thickness of the material in m

L = the length of the support legs in m

δ = the Boltzmann constant

ε = the effective emissivity of the material

A = the area of the entire device in m^2

Tm = the temperature in K

λ_{air} = the thermal conductivity of air in W/mK

d = the distance from membrane structure to cavity bottom in m

The gaseous thermal conductance calculations assume that the heat loss through the air above the membrane structure to the device package is negligibly small and therefore only the heat loss through the air beneath the structure is considered. Calculation performed by using equation 1 must be done for each layer used in the design as shown in figure 2, and then added together to calculate the total thermal conductance of the bolometer device.

Devices used for the support leg width test all have a membrane area of $900 \mu m^2$ and support legs of $30 \mu m$ long. The width of their support legs are changed in steps of $4 \mu m$ as shown in figure 3, where an increase in support leg

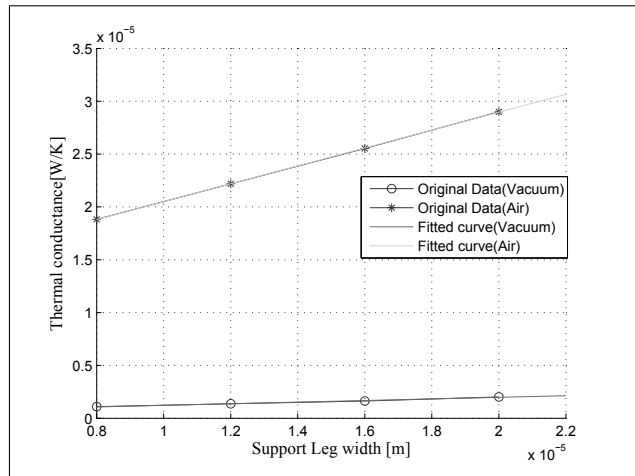


Figure 3: Thermal conductance of devices with support legs of $30 \mu m$ long

width produced an increase in thermal conductance. This increase in thermal conductance is caused by the increase in the thermal connection between the membrane and the anchors which increases the heat transfer speed.

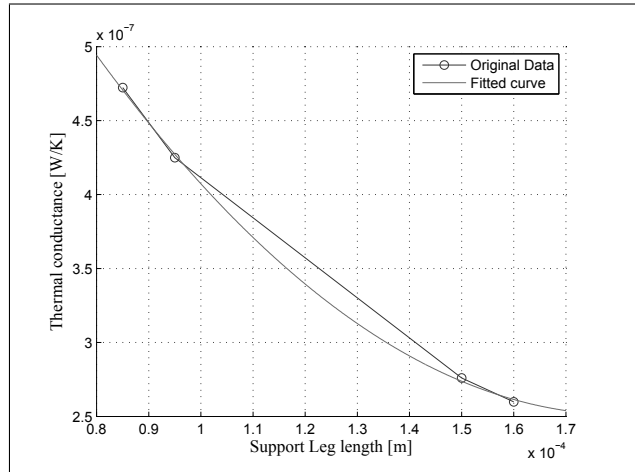


Figure 4: Thermal conductance of devices with support legs of $10 \mu m$ wide packaged in vacuum

Devices used for the support leg length test have a membrane area of $1600 \mu m^2$ and $10 \mu m$ wide support legs. The change in thermal conductance for test devices, with different lengths of support legs, packaged in vacuum and in air are shown in figure 4 and 5, respectively. Results indicate that in order to reduce the thermal conductance, the support legs must be shortened for devices packaged in air and lengthened for devices packaged in a vacuum. This difference is due to the large contribution of gaseous thermal conductance through the air beneath the support legs to the bottom of the cavity of the devices packaged in air.

Thermal capacitance is a measure of the microbolometer's heat retention ability. The thermal capacitance is only affected by the volume of the microbolometer device and therefore it can be assumed that when the total

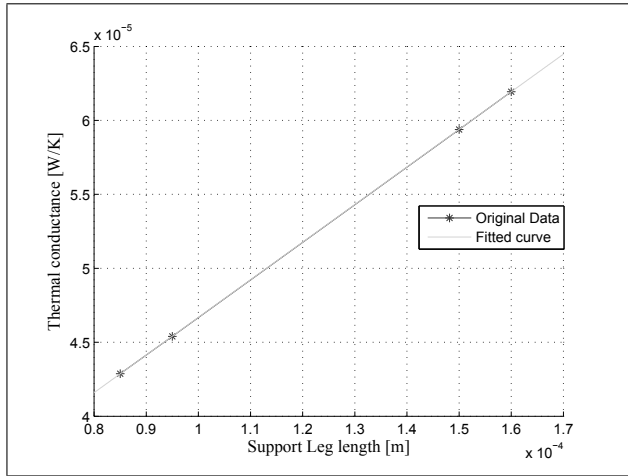


Figure 5: Thermal conductance of devices with support legs of $10 \mu\text{m}$ wide packaged in air

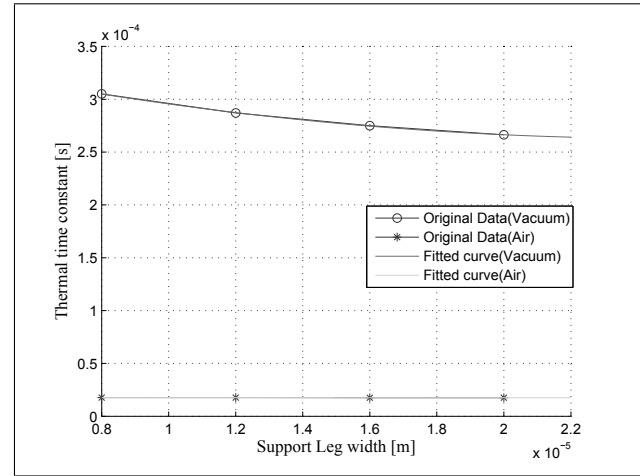


Figure 6: Thermal time constant of devices with a membrane area of $900 \mu\text{m}^2$

volume of the microbolometer is increased the thermal capacitance is also increased. Equation 2 is used to calculate the thermal capacitance of each layer of the microbolometer device. The thermal time constant can be calculated with equation 3 by using the total thermal capacitance and thermal conductance values calculated [4, 5]. The thermal capacitance and the thermal conductance are used together to determine the thermal time constant of a microbolometer device. This thermal time constant determines the maximum speed at which the microbolometer can operate. The readout circuit can limit the operating speed further but is not capable of reducing the thermal time constant beyond this value without altering the design layout.

$$H = V\rho c, \quad (2)$$

where:

V = the volume of the device m^3
 ρ = the density in g/m^3
 c = the specific heat in J/gK

$$\tau = \frac{H_{Total}}{G_{Total}}, \quad (3)$$

where:

H_{Total} = the total thermal capacitance of all the layers in J/K
 G_{Total} = the total thermal conductance of all the layers in W/K

Figure 6 shows the change in thermal time constant with a change in support leg width for the test devices used in the thermal conductance and thermal capacitance calculations above. Figure 7 and 8 show the thermal time constant with a change in support leg length for test devices used above packaged in a vacuum and in air, respectively.

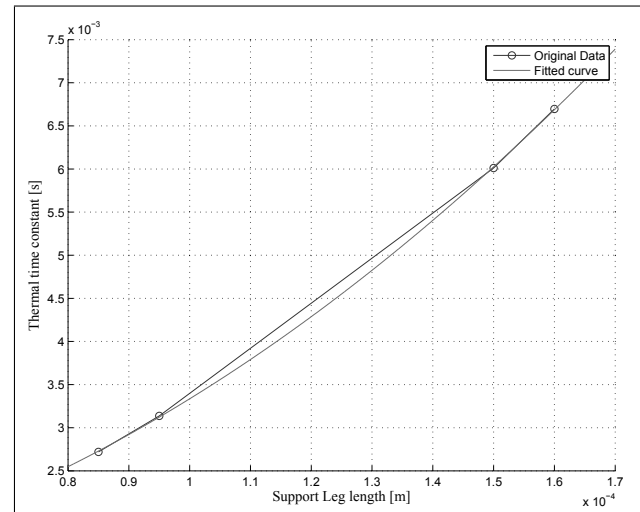


Figure 7: Thermal time constant of devices with support leg widths of $10 \mu\text{m}$ packaged in vacuum

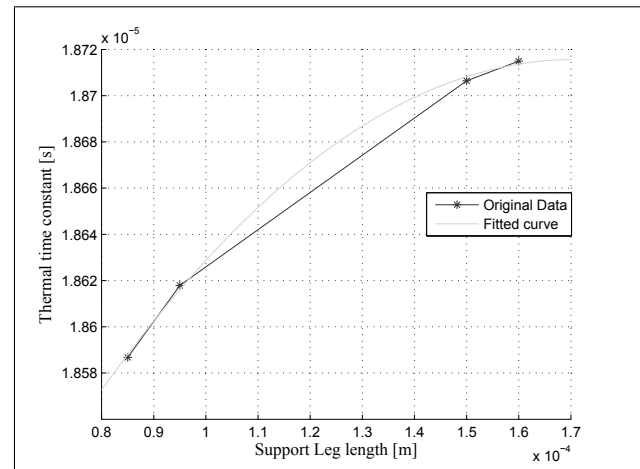


Figure 8: Thermal time constant of devices with support leg widths of $10 \mu\text{m}$ packaged in air

4. PREDICTION AND OPTIMISATION OF THERMAL PROPERTIES

Microbolometers are designed to have a specific time constant. This time constant can be adjusted to improve the performance of a device by altering its structural layout [6]. The previous sections show simulation results for devices where different structural dimensions are varied to isolate the change in thermal time constant to a specific structural dimension.

Results shown in the previous sections indicate that the time constant for bolometer devices can be lengthened by increasing the length of the support legs, or alternatively reducing the width. By using the results shown in figures 3 to 5 and the thermal capacitance values calculated with equation 2 for the same devices, equations 4 to 6 can be derived. These equations can be used to calculate the expected thermal conductance and thermal capacitance values for devices based on basic structural dimensions. These predicted thermal conductance and thermal capacitance values are then used to estimate the thermal time constant of a device by using equation 3.

$$\begin{aligned} G_{Air} = & 0.187L_{Leg} + 1.28 \times 10^4 A_{Mem} \\ & + 0.85W_{Leg} - 6.812 \times 10^{-6} \end{aligned} \quad (4)$$

$$\begin{aligned} G_{Vac} = & 53.3L_{Leg}^2 - 0.023L_{Leg} + 0.076W_{Leg} \\ & - 16.37A_{Mem} + 1.1586 \times 10^{-6} \end{aligned} \quad (5)$$

$$H = 0.483W_{Leg}L_{Leg} + 0.528A_{Mem} \quad (6)$$

where:

L_{Leg} = the length of the support legs in m

W_{Leg} = the width of the support legs in m

A_{Mem} = the area of the membrane structure in m^2

Equations 4 to 6 make use of the basic structural dimensions to estimate the thermal performance of a microbolometer device. These equations are only valid for devices manufactured with the layers shown in figure 2 with Vanadium Oxide used as sensing material.

5. THERMAL PROPERTY VERIFICATION OF MANUFACTURED DEVICES

Manufactured microbolometers differ slightly from their designs due to variations in material thickness and device deformation. Deformation of a bolometer device usually causes the distance between the device membrane and the cavity bottom to change, this affects the thermal conductance of devices packaged in air.

Manufactured test devices can be used to calculate the actual distance between the membrane and the cavity bottom if deformation is suspected. Figure 9 shows the thermal conductance calculated from experimental measurements of test devices with different membrane sizes [4, 7].

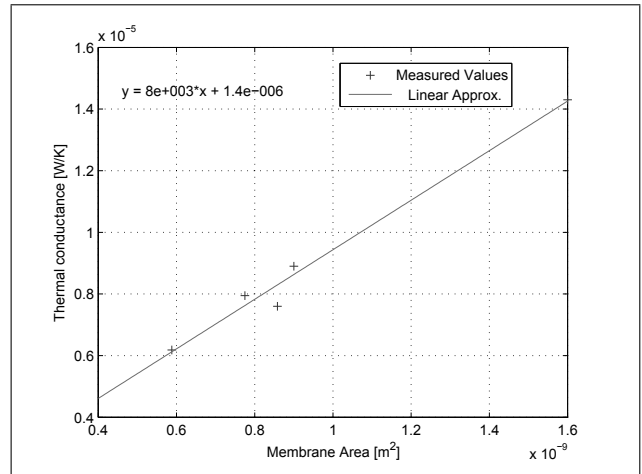


Figure 9: Thermal conductance with a change in membrane area

The actual distance between the membrane and the cavity bottom can be calculated by using the slope of the linear curve fitting shown in figure 9 and equation 7 below.

$$G_{atm} = \lambda_{air} \frac{A}{d}, \quad (7)$$

where:

λ_{air} = the thermal conductance of air in $W/m.K$

A = the area of the sensing membrane in m^2

d = the distance between the membrane and the cavity bottom in m

Equation 7 shows that the slope of the linear curve shown in figure 9 represents the ratio $\frac{\lambda_{air}}{d}$, where λ_{air} is a known constant. It can therefore be calculated that the actual distance between the sensing membrane and the cavity bottom is $3.2\mu m$ and not $2\mu m$ as the design indicates in figure 2. This deformation could be as a result of internal stress between the layers used in the design which caused the membrane to bend upwards after the sacrificial layer was removed, or due to the increased temperature required during the final steps of manufacturing.

Material thickness and property variations can change the performance of the actual device and make performance predictions difficult. The thermal conductance of microbolometer devices packaged in a vacuum can be used to derive a constant which is independent of material thermal properties and layer thickness, limited to a specific design process. Figure 10 shows the thermal conductance of microbolometer devices as a function of the number of squares in their support legs. The number of squares in

a support leg is calculated by dividing the length of the support leg by its width. This shows the amount of equally sized square blocks needed to form all the support legs of a microbolometer device. These square blocks are made up of the layers used for the specific design process and are equal in thickness.

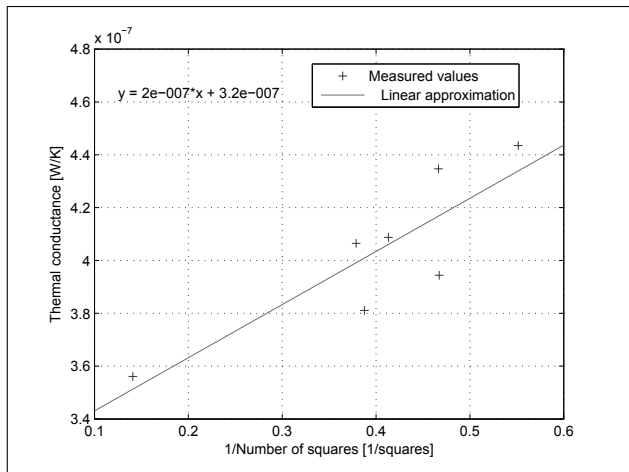


Figure 10: Thermal conductance with a change in the number of squares in the support legs

The physical thermal conductance shown in equation 8, is the major contributing factor of thermal conductance for devices packaged in a vacuum. The slope of the fitted curve shown in figure 10 is defined as the thermal conductance per square for the range of manufactured microbolometers. Substituting this newly derived thermal conductance per square value ($2 \times 10^{-7} \frac{W/K}{\#Squares}$) in equation 8 for $\frac{L}{W}$, leaves only two unknown variables, the thickness and thermal conductance of the materials in each layer. These variables are identical as shown in figure 2 for all the devices manufactured with the same process and can therefore be excluded.

$$G_{physical} = \lambda \left(\frac{WT}{L} \right), \quad (8)$$

where:

λ = the thermal conductance of each material in $W/m.K$
 W = the width of the support legs in m
 T = the thickness of each material m
 L = the length of the support legs in m

The thermal conductance per square can therefore be used to estimate the thermal conductance of any microbolometer device packaged in a vacuum based only on the amount of squares in their support legs as shown in equation 9.

$$G_{physical} = \left(\frac{G_{Squares}}{\#Squares} \right) + C, \quad (9)$$

$G_{Squares}$ = the thermal conductance per square in $\frac{W/K}{\#Squares}$
 $\#Squares$ = the amount of squares in the support legs in *amount*
 C = the minimum thermal conductance practically achievable in W/K

6. CONCLUSION

The thermal performance calculation of a microbolometer design can be simplified by using equations 4, 5 and 6 to predict the thermal conductance and thermal capacitance prior to building a sophisticated model or performing complicated calculations. These values can be used to calculate the expected thermal time constant and adjust the structural dimensions of the bolometer device to obtain the desired performance values. Calculation results used to derive the above mentioned equations can also be used to aid in making changes to the structure of the microbolometer to achieve the required thermal time constant.

Manufactured devices perform different from simulations due to unexpected structural deformations and process variations. Calculations shown are used to determine the amount of structural deformation of microbolometer devices, by using measured thermal properties. Equations are derived that can be used to simplify the estimation of thermal conduction calculations by eliminating the use of process dependant variables that are common to all devices. These calculations are limited to a set of devices manufactured on the same substrate or with the same processing steps.

7. ACKNOWLEDGEMENTS

The authors would like to thank the Advanced Manufacturing Technology Strategy (AMTS) of the Department of Science and Technology, South Africa for the financial support of the research.

8. REFERENCES

- [1] S. Gilmartin, D. Collins, D. Bain, W. Lane, O. Korostynska, A. Arshak, E. Hynes, B. McCarthy, and S. Newcomb, "Uncooled IR nanobolometers fabricated by electron beam lithography and a MEMS/CMOS process," in *8th IEEE Conference on Nanotechnology 2008*. IEEE, 2008, pp. 131–134.
- [2] Y. Tsujino, "An approach for the performance analysis of an uncooled infrared bolometer imager," *Infrared Physics and Technology*, vol. 53, pp. 50–60, 2010.
- [3] A. Rogalski, "Optical detectors for focal plane arrays," *Opto-electronics review*, vol. 12, pp. 221–245, 2004.
- [4] P. Eriksson, J. Andersson, and G. Stemme, "Thermal characterization of surface-micro machined silicon nitride membranes for thermal infrared detectors," *Journal of Microelectromechanical Systems*, vol. 6, pp. 55–61, 1997.

- [5] F. Niklaus, A. Decharat, C. Jansson, and G. Stemme, "Performance model for uncooled infrared bolometer arrays and performance prediction of bolometers operating at atmospheric pressure," *Infrared Physics and Technology*, vol. 51, pp. 168–177, 2008.
- [6] H. Najafabadi, A. Asgari, M. Kalafi, and K. Khalili, "An analytical model for detectivity prediction of uncooled bolometer considering all thermal phenomena effects," *Procedia Engineering*, vol. 8, pp. 280–285, 2011.
- [7] J.-S. Shie, Y.-M. Chen, and B. Chou, "Characterization and modelling of metal-film microbolometers," *Journal of Microelectromechanical Systems*, vol. 5, pp. 298–306, 1996.